ECOLOGY

Faster, bigger, more severe: Extreme wildfire spread sets the stage for forest ecosystem change in western and boreal North America

Jonathan D. Coop[1]*, Jared A. Balik[1], Jessika R. McFarland[1,2], Sean A. Parks[3]†, Kyle C. Rodman[4], Camille S. Stevens-Rumann[5], Meg A. Krawchuk[6], Cameron E. Naficy[6,7], Marc-André Parisien[8], Ellen Whitman[8]

A relatively small number of rapidly spreading wildfire events burn disproportionately large areas. But beyond area burned, do fast fires produce distinct postfire ecological outcomes? Here, we measure daily linear fire growth rates and assess relationships between fire spread, burn severity, and metrics of postfire landscape resilience from 3499 fires occurring between 2012 and 2023 in conifer-dominated forests of Canada and the western US. We find that as linear spread rate increases, so too does fire severity, proportion of area burned at high severity, and distance to surviving live tree seed sources. Thus, not only do the fastest fires burn outsized areas, but these areas have less remaining tree cover and reduced capacity for recovery, setting the stage for long-term vegetation shifts. Given anticipated increases in extreme fire spread as fire seasons lengthen and weather becomes more fire-conducive, our findings highlight growing needs to effectively reduce undesired impacts, manage postfire landscapes to sustain forest ecosystem functions, and foster social-ecological adaptation.

INTRODUCTION

Record-breaking fire seasons have called attention to changes in measures of wildfire behavior including rates of fire growth (*1*). Extreme wildfire events, characterized by rapid expansion, exceptional behavior, and difficulty of suppression, are becoming more frequent (*2*, *3*). Just a small subset of fires account for the majority of infrastructure loss, economic costs, and lives lost (*4*). Rapidly growing fires also contribute disproportionately to patterns of annual area burned (*5*). For example, the top ~3% (>2 SD larger than the mean) of daily fire spread events accounted for up 37% of total area burned in forested ecoregions of the US and Canada 2002–2021 (*6*). Recent studies have quantified fire growth rates by area burned over daily or subdaily periods (e.g., ha/day), but fire progression maps can also be used to directly measure linear fire rate of spread (ROS; e.g., m/day), with opportunities to shed new light on what factors control fire growth rate (*7*, *8*), and potentially also how ROS might relate to fire effects.

Do "fast" fires burn more severely? Fire severity, as quantified by field- and satellite-derived measures [e.g., the composite burn index (CBI)], is a measure of fire's ecological effects, and is closely linked to fuel consumption (*9*). Byram's (*10*) equations show how total fire intensity increases with ROS, but fuel consumption and ROS are assumed to be independent (*11*). The fastest-growing fires in the US, as measured by daily area burned, occur in grasslands (*4*), where fire's ecological impacts are typically low due to relatively low fuel loads, rapid resprouting, and quick recovery of aboveground biomass. However, in forested landscapes, the fastest-moving fires are typically running crown fires that spread horizontally through tree crowns under strong winds and low fuel moisture (*12*, *13*). Because crown fires consume tree canopies, they are generally lethal to trees in most North American conifer forests (*14*) and have the potential to produce postfire landscapes with large, severely burned patches (*15*). Recent studies in some regions have found positive relationships between area burned and fire severity across scales (*16*–*19*). Further, as annual area burned increases, so too does the annual proportion of high-severity fire (*20*).

High-severity fire necessarily entails major short- and long-term consequences for ecological components and processes, including lost habitat for some species, reduced carbon storage, and altered hydrology (*21*, *22*). In forest types characterized historically by frequent, low-severity fire (e.g., ponderosa pine, *Pinus ponderosa*), the area burned at high severity within recent wildfire footprints is historically anomalous (*23*), leading to regional losses of mature forests (*24*). Even in forest types characterized by severe but infrequent fire (e.g., high-elevation or high-latitude pine and spruce forests), recent increases in high-severity fire may be approaching or exceeding historical norms (*25*, *26*). For plant species whose regeneration is dependent on live seed sources, large high-severity patches increase the distances that seeds must disperse, slowing recolonization (*27*–*29*). Further, the growing divergence between postfire climates and the historical conditions that gave rise to present forests can reduce tree seedling establishment and survival (*30*, *31*). Together, the loss of mature forest and decreased regeneration capacity can produce enduring shifts to alternate states and nonforest vegetation types, with major implications for a range of species and ecosystem functions (*32*). Accordingly, improving our understanding of relationships between wildfire behavior and ecological outcomes can help forecast change and inform management actions.

The goal of this study is to assess relationships between fire speed and associated ecological impacts to western and boreal North American conifer forests (Fig. 1). Within any given wildfire, we sample activity within single-day increments (referred to here as daily fire

[1]Clark School of Environment and Sustainability, Western Colorado University, Gunnison, CO, USA. [2]Department of Environmental Science, Policy, and Management, University of California Berkeley, Berkeley, CA, USA. [3]Aldo Leopold Wilderness Research Institute, Rocky Mountain Research Station, USDA Forest Service, Missoula, MT, USA. [4]Ecological Restoration Institute, Flagstaff, AZ, USA. [5]Colorado Forest Restoration Institute, Forest and Rangeland Stewardship, Colorado State University, Fort Collins, CO, USA. [6]Department of Forest Ecosystems and Society, Oregon State University, Corvallis, OR, USA. [7]GreenFire Geomatics, LLC, Missoula, MT, USA. [8]Northern Forestry Centre, Canadian Forest Service, Natural Resources Canada, Edmonton, Alberta, Canada.
*Corresponding author. Email: jcoop@western.edu
†Present address: Ariel Re UK Limited, London, UK.

spread events) to ask: how disproportionate are the effects of "fast" events, as measured by the maximum linear distance a fire travels each day it burns, on postfire conifer forest persistence and recovery potential? We draw from a dataset of ~3500 fires, representing ~33,600 daily fire spread events, that together burned 43 million ha between 2012 and 2023 in the western US and Canada. Specifically, we assess how daily linear ROS relates to (i) area burned, (ii) mean burn severity, (iii) proportion of area burned severely (CBI ≥ 2.25; ≥95% canopy mortality), and (iv) distance from high-severity patch interiors to live conifer seed sources.

RESULTS

Across the study area, the total area burned in sampled fires was 43.2 million ha between 2012 and 2023 (Table 1). Of this, the total area of conifer forest burned was 32.1 million ha, with over a third (11.2 million ha) burning at high severity. Day-of-burning (DOB) patch area, the area burned within a 24-hour period by a given fire, ranged from 25 to 141,257 ha and daily linear spread distances ranged from 131 to 61,878 m. The 10 fastest growing daily fire spread events (or 0.03% of all 33,594 events), each of which traveled >32 km within a 24-hour period, collectively burned 547,000 ha of conifer forest, with 50% burning at high severity (CBI ≥ 2.25). Of these events, seven occurred in Canada in 2023 and two occurred in the western US in 2020. By contrast, an equal area of 547,000 ha of conifer forest was burned by the slowest 42% of events (14,281 events), with only 25% of that area burned at high severity. Similarly, the fastest 1 and 10% of events burned 5.3 Mha (17% of total) and 16.8 Mha (52%) of conifer forest, with 42 and 39% burned at high severity; the slowest 50% of events burned 3.1 Mha (10%), with only 25% burned at high severity.

We found that ROS was closely related to DOB patch area (marginal $R^2 = 0.70$ and $P < 0.001$; Fig. 2A) and the maximum linear ROS exhibited by any given wildfire also strongly predicted the final total fire size (marginal $R^2 = 0.66$ and $P < 0.001$; Fig. 2B). Daily linear ROS was also positively related to measures of fire impacts to forest ecosystems. Daily spread events categorized as fast (representing fires with a linear spread rate exceeding the ecoregional mean + 1 SD; Table 1) burned 13% more severely (mean CBI = 1.94) than slow events (mean CBI = 1.72; $P < 0.001$; Fig. 3A), and ROS was positively related to burn severity ($P < 0.001$; Fig. 3B). Fast events also exhibited a greater proportion of area burned at high severity (34% versus 26%; $P < 0.001$; Fig. 3C) and greater distances from severely burned pixels to likely live-tree seed sources, measured by mean distance from high-severity patch interiors pixels to conifer forest pixels that had not burned at high severity (150 m versus 121 m, or an increase of 23%; $P < 0.001$; Fig. 3E). Both high-severity proportion and $\log_{10}$-distance to seed source were positively related to linear ROS ($P < 0.001$; Fig. 3, D and F). Linear ROS produced better fitting models than daily area burned for models predicting burn severity (AIC = −666,778 versus −663,237, respectively) and seed source distance (AIC = 987,329 versus 993,112). However, models predicting the proportion of high severity fire using linear ROS were weaker than those using daily area burned (AIC = −50914 versus −51901).

We examined patterns of ecoregional variation as a random effect on the intercept and slope of models relating burn severity, high severity proportion, and seed source distance to ROS (Fig. 4 and tables S1 to S3). These terms were statistically significant in each model. Relationships were broadly consistent across ecoregions. In general, warmer and drier ecoregions (e.g., Mediterranean California and Upper Gila Mountains) had reduced fire effects relative to cooler and wetter ecoregions (e.g., Marine West Coast Forest). While most

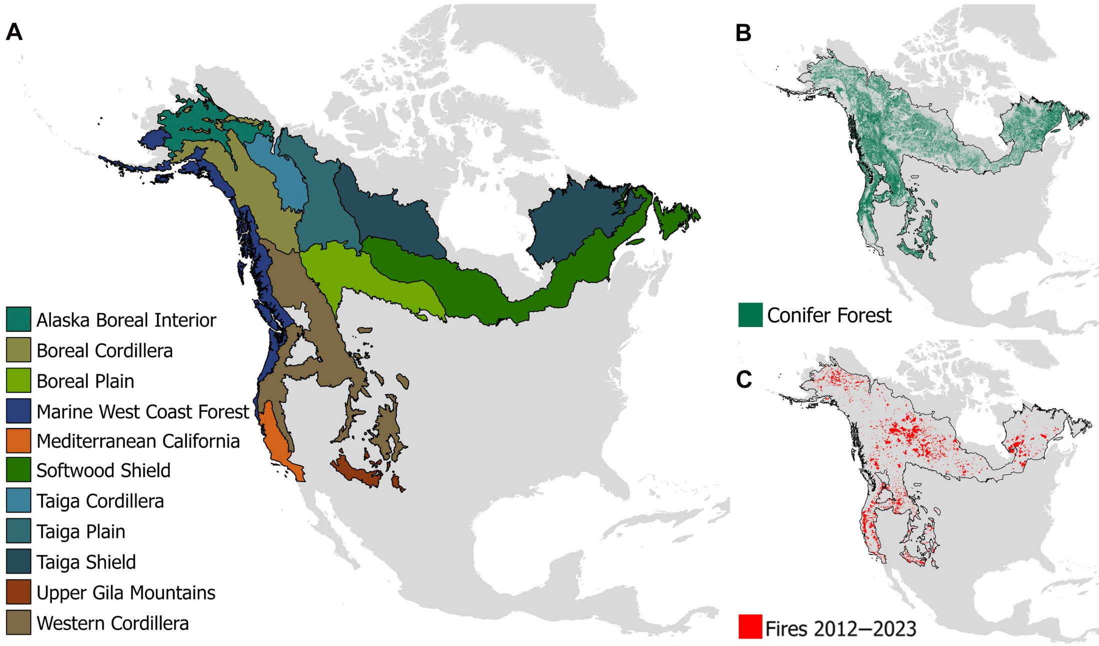

Fig. 1. Study area. (**A**) Eleven North American US EPA Level 2 Ecoregions, (**B**) conifer forest pixels at the beginning of the study period based on Landfire (USA) and Hermosilla *et al.* (*78*) (Canada), and (**C**) fires >400 ha from Monitoring Trends in Burn Severity (MTBS; USA) and the National Burned Area Composite (NBAC; Canada), occurring 2012–2023.

Table 1. Summarized fire activity for each US EPA level 2 ecoregion, 2012–2023. Total area burned, conifer forest area burned, number of fires and daily fire spread events, the linear ROS threshold (m/day) used to identify fast daily fire spread events (>mean + 1 SD), and the proportion of area burned by fast events.

Ecoregion	Area burned (ha)	Conifer forest area burned (ha)	Fires (n)	Daily fire spread events (n)	Fast daily fire spread events (n)	Fast fire threshold (m/d)	Proportion of total area burned by fast events
Alaska Boreal Interior	3,723,431	2,768,794	329	2930	461	3879	0.52
Boreal Cordillera	1,171,017	902,327	163	1416	234	3225	0.55
Boreal Plain	2,929,749	1,919,380	149	1266	215	4950	0.70
Marine West Coast Forest	280,051	207,141	39	313	52	2914	0.66
Mediterranean California	1,650,517	715,285	148	717	108	5059	0.58
Softwood Shield	6,902,859	5,263,956	498	4428	748	4184	0.67
Taiga Cordillera	229,622	179,128	49	412	60	2661	0.50
Taiga Plain	6,458,042	4,269,067	301	3382	530	4269	0.68
Taiga Shield	7,072,374	5,695,744	424	4258	656	3742	0.66
Upper Gila Mountains	1,263,860	987,565	179	1178	189	3302	0.55
Western Cordillera	11,568,242	9,211,001	1220	13,294	1952	2835	0.61
Study area total	43,249,764	32,119,387	3499	33,594	7648	NA	0.63

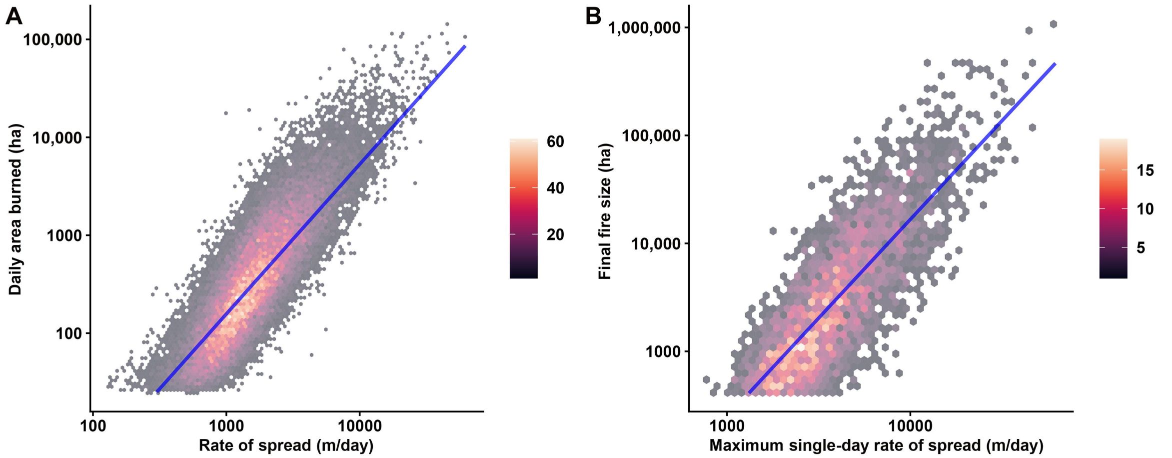

Fig. 2. Fire ROS is closely related to area burned. Relationships of main effects of linear mixed-effects models between (**A**) daily linear ROS and daily area burned (marginal $R^2 = 0.70$) and (**B**) the maximum linear spread exhibited during the life of a fire and its final size (marginal $R^2 = 0.66$). Both models' intercepts and slopes were significant at $P < 0.001$. Sample density is represented by the dark to light color in hexagonal bins [total $n = 33,594$ DOB patches in (A); 3499 fires in (B)]. The blue lines show the model fits.

slopes were similar, those of the Western Cordillera increased more steeply than other ecoregions in each model, and those of the Boreal Plain were shallower.

DISCUSSION

Here, we relate linear fire ROS to fire effects on forest landscapes and shed light on the compounding ecological impacts of fast-moving fires: Not only do they burn more area but they also burn that area more severely. It is well understood that aggregate measures of fire effects such as economic losses and area burned reflect the outsized influences of a small subset of the most extreme wildfires (*4*, *5*, *33*, *34*). The relationships we identify here, between ROS, area burned, and fire severity, scale from the individual DOBs to wildfires and likely underpin relationships between total area burned and burn severity over entire fire seasons (*20*). Despite geographic variation in fire progression and its controls (*6*, *35*), the relationships we identified were consistent across western and boreal conifer-forest dominated ecoregions of North America. As climate change continues to increase forest fuel flammability (*36*), fire season duration (*37*), and the likelihood of weather conducive to extreme wildfire (*38*, *39*), we anticipate further expansion of fast daily fire spread events. Such

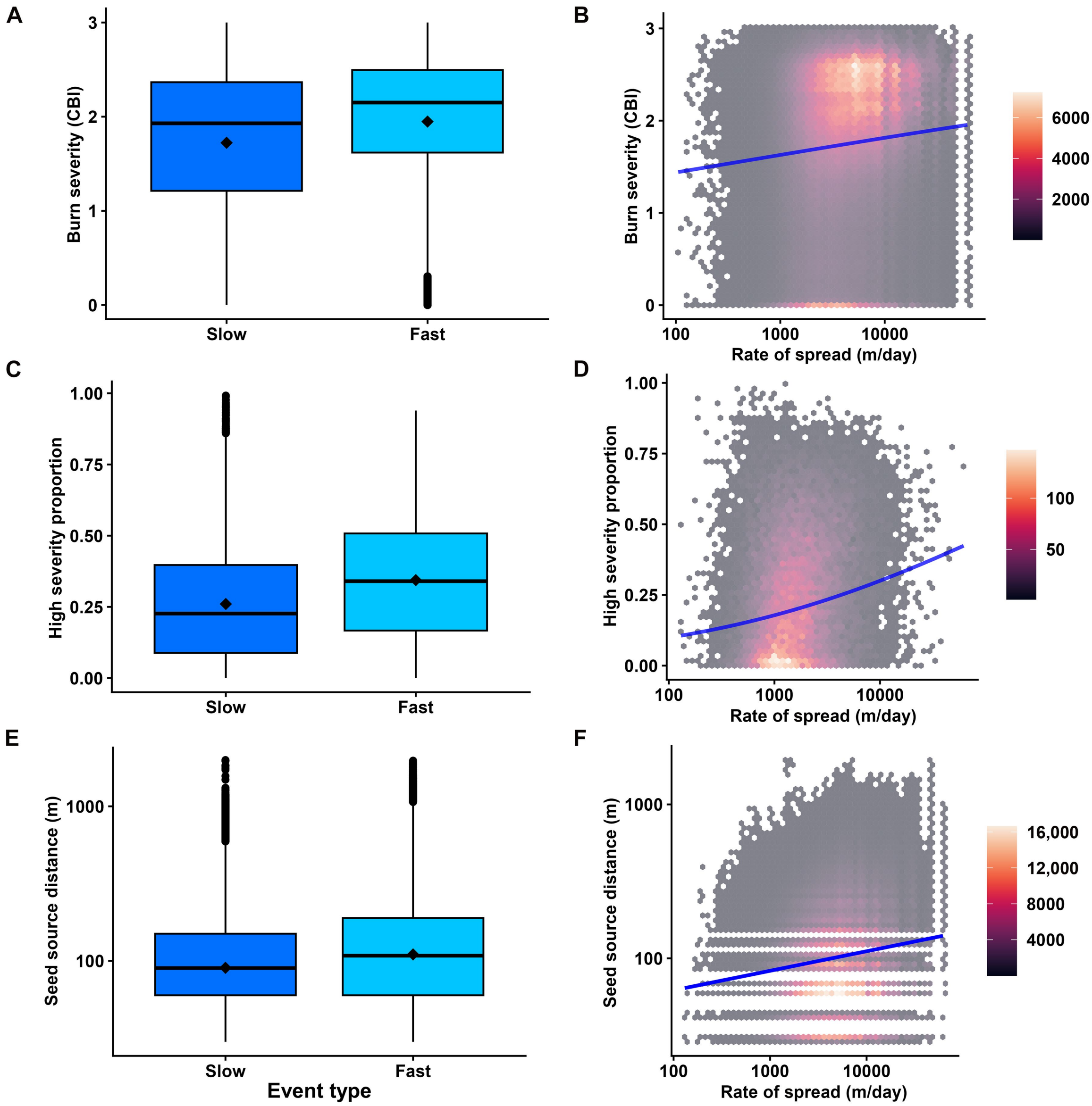

Fig. 3. Fire ROS predicts effects to forest landscapes. Relationships between daily fire spread event types (slow or fast) and maximum daily linear ROS (m/day) and fire effects in study area conifer forests including (**A** and **B**) burn severity (Composite Burn Index, CBI), (**C** and **D**) proportion of event area burned at high severity (CBI ≥ 2.25), and (**E** and **F**) distance to conifer seed source, as measured by the linear distance from high severity patch interior to the closest non–high-severity conifer pixel (m). In all boxplots [(A), (C), and (E)], the median value is represented by the horizontal black line, the mean by the black diamonds; all differences between slow and fast events were highly significant, $P < 0.001$. Blue trendlines [(B), (D), and (F)] show estimates of main effects from linear (D) and generalized linear [ordinal beta, (B) and (F)] mixed effects models. All model intercepts and slopes were highly significant, $P < 0.001$. The dark-to-light hexagonal bin color ramp represents the density of samples [total $n = 2.7 \times 10^6$ pixels in (B), 2.5×10^6 pixels in (F), 3.3×10^4 DOB polygons in (D)].

events will challenge the resilience of conifer forest ecosystems throughout North America and other temperate biomes.

Fire weather and fuel availability are two important controls on fire behavior that mechanistically tie ROS to severity and could produce the relationships identified here. Wind speed is positively related to fire growth (*40*), crown fire (*41*), and large, aggregated high-severity patches (*42*). Fuel moisture is also a strong predictor of fire behavior: Drier fuels promote greater fuel consumption and radiative energy release (*43*) and can lower barriers to fuel connectivity (*33*), increasing both fire severity and ROS. Positive feedbacks can also amplify these attributes of fire behavior. For example, canopy fuel consumption in active crown fires exposes the flaming front to ambient winds, increasing ROS (*44*). Further, highly fire-conducive fuel and atmospheric conditions can foster self-organizing fire behavior including mass fire (*45*), pyrocumulonimbus formation (*46*), and pyrotornadogenesis (*47*), each of which can increase ROS or fuel consumption. In contrast, lower wind speeds, high fuel moisture, and/or discontinuous canopy fuels associated with topographic variation or ecologically heterogeneous landscapes can reduce ROS and produce mosaics of varying burn severity that incorporate areas

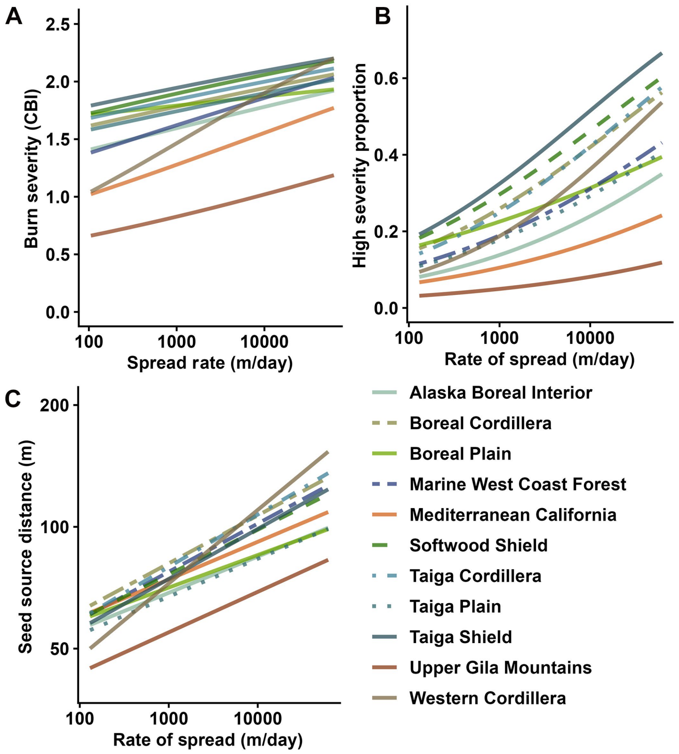

Fig. 4. Ecoregional influences on relationships between daily ROS. (**A**) Burn severity, (**B**) proportion of area burned at high severity, and (**C**) distance from high-severity patch interior to conifer forest burned at CBI < 2.25. Trendlines represent the random effect terms of each ecoregion added to the intercept and slope of the main effect.

of low-severity surface fire and unburned patches as fire refugia (*48*, *49*).

High-severity fire reshapes forest ecosystems and alters a range of habitat values, carbon stocks, and other ecosystem services. For example, irreplaceable giant sequoias (*Sequoiadendron giganteum*) were killed at uncharacteristically high rates by recent, severe wildfires in California (*50*). Because regeneration by many western North American tree species is dependent on seed dispersal by wind from mature, live tree seed sources, postfire recovery rates are constrained where the interiors of burned patch interiors are far from surviving trees (*31*, *51*). The 30-m resolution of this study is likely to lead to overestimation of surviving conifer seed source distances due to a minimum measurable distance of 30 m and because severely burned pixels can still contain some surviving trees (*52*). Nevertheless, it is apparent that as fire spread rate increases, so too does the area of high-severity fire and the distance to surviving tree seed sources. Tree species of forest types that were historically characterized by infrequent but severe fire (e.g., lodgepole pine, *Pinus contorta var. latifolia*, and black spruce, *Picea mariana*) have adaptations such as cone serotiny that facilitate regeneration following lethal fire (*53*) and might increase in dominance in the face of more severe wildfire (*54*, *55*). However, although serotinous species with aerial seed banks do not necessarily require live-tree seed sources to regenerate, intense crown fire may still reduce seed viability, and even these species often show declining regeneration success with increasing distance into high-severity patches (*56*, *57*). In some settings, aspen (*Populus tremuloides*) may be particularly well-poised for expansion given both rapid resprouting but also very long-distance seed dispersal (*58*). Similarly, resprouting shrubs such as Gambel oak in the southwestern US (*59*) may become more dominant where severe fire removes conifer seed sources from large landscapes.

Ecoregional variation in relationships between fire ROS and landscape effects appears to reflect differences in forest fuel availability. More arid southern ecoregions including the Upper Gila Mountains and Mediterranean California exhibited lower burn severity and proportion burned severely than the more mesic boreal ecoregions, likely due to lower total aboveground biomass associated with open, dry forest stand structure. Live fuel load is consistently identified as the most important single determinant in models predicting fire severity (*60*, *61*). While modeled slopes were broadly consistent across ecoregions, the steeper relationships between ROS and fire effects (including CBI, high-severity proportion, and seed-source distance) in the Western Cordillera are notable. This ecoregion contains the broadest range of forest types and is characterized by strong elevational gradients in forest aboveground biomass, with sparse fuels in open forests at lower elevations contrasting with fuel-rich, continuous montane and subalpine forests at higher elevations. It may be that slower ROS here is more strongly associated with open forest (similar to effects in arid southern ecoregions) but faster ROS is associated with closed forests (similar to effects in fuel-rich boreal ecoregions). The Western Cordillera is also likely to have experienced the greatest effects of ongoing modern fire suppression, which alters the distributions of area burned across a gradient of fireline intensity and resulting patterns of fire severity [i.e., the "fire suppression bias;" (*62*)]. Less intense prescribed fire and managed wildfire may be allowed to burn under conditions where spread is slow and burn severity is low, but most area burns under extreme conditions when suppression is ineffective, ROS is fast, and severity is high.

Given relationships between fire ROS and ecological effects, as climate becomes increasingly conducive to fast, big, and severe wildfires, we can anticipate growing impacts to the conifer forests of the western mountains and the boreal biome of North America. Beyond the immediate effects of such fires on forest ecosystems, they may produce enduring landscape changes that are compounded by a changing climate. Warming and drying conditions, acting alone or in combination with postfire limitations on seed availability, can also reduce the likelihood of postfire recovery of prefire conifer forest types (*63*, *64*). Where these mechanisms tip conifer forest systems toward alternate states, there are a wide range of implications for ecosystem functions including carbon storage, albedo, and hydrology. In some settings, such changes may produce feedbacks that could inhibit future fire activity, for example by reducing fuel availability in recent burns (*65*, *66*) or where conifer forests shift towards less flammable broadleaf forest types (*8*). Vegetation changes can also promote fire activity, such as is observed where fire produces faster growing grass or shrub species that add to available fuel in early postfire periods (*67*). However, changes in fire activity imparted by such shifts may be negated by warming and drying. For example, while fire progression is limited by recent prior burns, relatively small increases in fire-conducive weather can overcome these limitations (*68*).

Because fast-moving fires generally occur under conditions that reduce the effectiveness of wildfire incident management (for example, when strong winds preclude aviation or limited resources and assets may already be deployed to multiple large incidents), prefire planning and proactive fire management is essential to mitigating undesired outcomes to people and forests alike. Such actions necessarily entail community preparedness including adequate warning and evacuation procedures (*69*). Human communities face increasing risks including economic and health burdens such as wildfire-initiated urban conflagrations, increased insurance costs, and exposure to particulate pollution from smoke (*70*). Fire incident management may also need to use adaptation responses to fire behavior and impacts under future climate (*71*). Reducing undesired impacts to forested landscapes requires a wide range of measures that reduce fire spread and/or severity. These include the restoration of low-severity fire regimes via thinning treatments followed by prescribed or managed fire (*72*) where ecologically appropriate (e.g., frequent-fire forest types) and socially acceptable. Promoting heterogeneous landscape mosaics that include large patches of low-fuel or fire-resistant vegetation may be more useful in mitigating fast-burning fire. For instance, management actions could expand less-flammable broadleaf forest types such as trembling aspen (*P. tremuloides*) through silviculture, prescribed fire, or wildfire managed under moderate burning conditions (*8*, *73*) in some infrequent-fire subalpine and boreal forest types. Understanding locations where live tree refugia are most likely to persist (*49*) through extreme events may also support management actions that can enhance forest resistance and postfire recovery. Last, expanded capacity to reforest severely burned landscapes, including assisted migration of tree species and assisted gene flow of populations suited to future climate, will likely be needed to restore and maintain vulnerable forest landscapes across portions of our study region (*74*).

Our study highlights the use of satellite-measured daily linear fire ROS, but we also acknowledge limitations to our approaches. By calculating linear ROS from satellite detections, we provide a measure of fire speed that can link foundational models of fire spread (*75*) to fire activity at the scale of large landscapes. Examining daily linear spread also offers benefits over daily area burned for studying wildfire with operational applications in mind. Linear ROS can better distinguish between fast versus slow spread (important for suppression and safety) independent of fire size: large fires can have an extensive, active perimeter than produces large daily area burned but with relatively slow ROS. However, the tight relationship between one-dimensional linear ROS and two-dimensional area burned suggests that for some purposes, the additional effort required to measure linear growth may not be needed. We also note, as an important limitation, that calculating ROS with DOB polygons is spatially and temporally coarse, undoubtedly masking considerable fine-scale variation that could be informative—within a given polygon, not every pixel burned at our calculated ROS. Higher-resolution methods that measure ROS at the pixel rather than the polygon scale, or sample at subdaily intervals, could facilitate an improved understanding of the drivers and outcomes of fast fire spread at management-relevant scales (e.g., determinants of early, explosive fire growth, or effectiveness of firelines and fuel treatments in slowing fire growth).

Despite of escalating expenditures for fire and forest management, fire activity continues to increase in western and boreal forests of North America under an increasingly fire-conducive climate. Without globally effective climate mitigation that includes rapid reductions in greenhouse gas emissions, future warming can be expected to drive growth in fire impacts to valued conifer forests and other critical ecosystems far into the future. We can anticipate a range of consequences, both good and bad in relation to human values, to ecosystem services such as timber products, water yield, wildlife, and recreation. These compel not just management attention but will also demand social adaptation to altered landscapes and ecological processes.

MATERIALS AND METHODS

Study area, forest masking, and wildfire perimeters

Our study area encompasses recent wildfires in conifer forests of Canada and the western United States (Fig. 1). We selected the following 11 North American Level 2 Ecoregions (*76*) for analysis: Alaska Boreal Interior, Boreal Cordillera, Boreal Plain, Marine West Coast Forest, Mediterranean California, Softwood Shield, Taiga Cordillera, Taiga Plain, Taiga Shield, Upper Gila Mountains, and Western Cordillera (Fig. 1A). Within this study area, we focus on conifer-dominated forests (Fig. 1B) burned in recent wildfires (2012–2023; Fig. 1C). To restrict our analyses to coniferous forests, we masked nonconifer pixels (30-m resolution) using LANDFIRE Existing Vegetation Type [EVT; (*77*)] data for the United States and the disturbance-informed annual land cover classification for Canada (*78*). Specifically, we reclassified LANDFIRE EVT pixels labeled as coniferous or mixed-conifer forest into a binary mask distinguishing conifer-dominated from nonconifer areas. For each year of fire occurrence, we used the most recent LANDFIRE product as a binary mask. For Canada, we retained prior-year pixels classified as coniferous forest and reclassified all other vegetation types to nonconifer. Wildfire perimeters were obtained from monitoring trends in burn severity (MTBS) for the US (*79*) and from the National Burned Area Composite (NBAC) for Canada (*80*). Prescribed fires and fires that did not overlap with conifer pixels were excluded from analysis. The centroid of each perimeter was used to assign burns to specific ecoregions.

Calculating daily fire spread and postfire landscape metrics

We developed maps of spatially continuous DOB patches by interpolating fire detections for 3499 fires ≥400 ha that burned between 2012 and 2023 (Fig. 5), following previously developed methods (*6*, *81*). We first obtained Moderate Resolution Imaging Spectroradiometer (MODIS) and Visible Infrared Imaging Radiometer Suite (VIIRS) fire detections (https://firms.modaps.eosdis.nasa.gov/map/) for Canada and the US. We limited our analysis to fires with ≥10 satellite thermal anomaly detections. We assigned detections to individual days using a 24-hour period beginning at 0600 hours and ending at 0559 hours local time the following day, assuming that most nighttime detections represent lingering heat from the prior day. DOB interpolations were produced at a 30-m spatial resolution, matching the resolution of the conifer forest mask and fire severity data, and constrained to the final mapped fire perimeter from MTBS or NBAC.

We were interested in exploring linear ROS, rather than daily area burned, as a metric of wildfire behavior that might predict fire impacts. In particular, we sought to characterize DOB patches by the maximum distance the fire traveled on that DOB, following the methods of Harris *et al.* (*8*). To calculate ROS, we first identified shared boundaries between chronologically sequential DOB patches. We then rasterized the distance from the beginning of each day's spread (its boundary with the previous day) to the end of that day's spread (the remaining perimeter). In cases where there was no shared boundary (such as for the first DOB patch of each fire, spread originating from a spotfire, or spread following gaps of 1 or more days in fire progression) distance was rasterized from the earliest hotspot detection within the DOB patch to the patch perimeter. From these

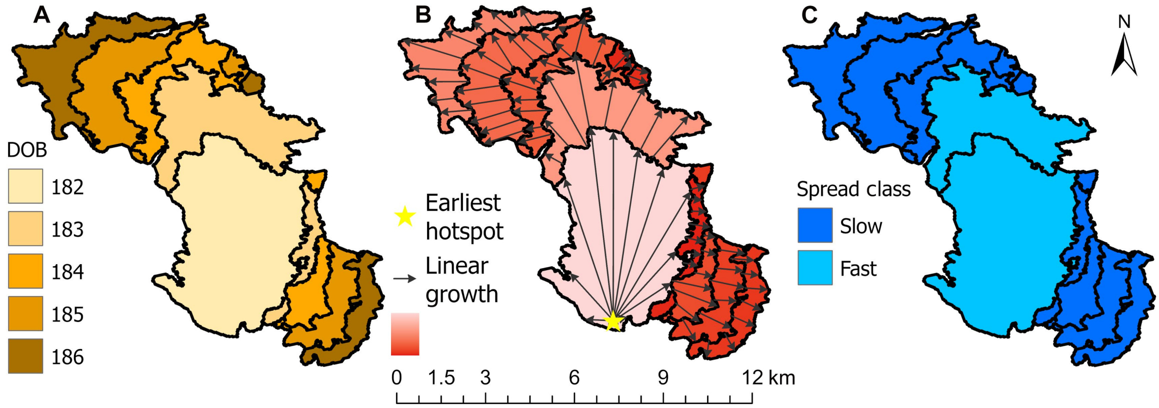

Fig. 5. Overview of methods to calculate daily ROS. Illustration of mapping (**A**) day-of-burning (DOB), (**B**) daily linear growth (ROS), and (**C**) categorization of "fast" versus "slow" daily fire spread events. DOB maps are interpolated from MODIS and VIIRS fire detections; ROS is the greatest distance from the point-of-origin or previous day's boundary the subsequent day's perimeter; classification is based on ecoregional thresholds (slow fires < mean + 1 SD; fast fires >mean + 1 SD).

rasterized distances, we determined the maximum linear distance traveled within any DOB patch. We assigned that value to the entirety of the area burned for that day. Last, we classified DOB patches as fast when their fire spread rate was greater than or equal to a threshold representing the mean + 1 SD of all daily fire spread rates measured in each ecoregion (Table 1 and Fig. 5) and slow when it fell below that threshold. We refer to these classified DOB patches as representing fast and slow spread events. The use of an ecoregional threshold recognizes variation in typical fire sizes and fire behavior among ecoregions; what constitutes an extreme event in one ecoregion might be considered common in another (*6*). In total, we measured daily area burned and ROS for 33,594 daily fire spread events. Models described below predict fire effects using both the continuous daily linear ROS but also a binary classification of DOB patches as either fast or slow (Fig. 5).

We quantified burn severity as the predicted CBI derived from Google Earth Engine (*82*) and the Random Forest model developed by Parks *et al.* (*83*). This model estimates field-measured CBI from pre- and postfire Landsat imagery, climate, and latitude at a 30-m resolution. CBI represents effects of fire on soils, surface fuels, and vegetation and ranges from 0 (unburned) to 3 (most severe) (*84*). We applied the conifer forest mask described above to the CBI rasters, retaining only conifer-dominated pixels for further analysis of burn severity in conifer forests, and sampling 0.1% of these pixels at random to reduce pseudoreplication and increase computation speed. We defined high-severity fire as CBI ≥ 2.25, which corresponds to ≥95% canopy mortality (*85*). The proportion of high severity was calculated as daily area burned at high severity over the DOB patch area. We calculated distance from high-severity patch interiors to the closest conifer live tree seed source as the distance between a random sample of 0.1% of points within each high-severity patch and the closest pixel containing conifer forest outside of the fire perimeter or with CBI < 2.25 (unburned to moderate severity) within the fire perimeter. The 30-m resolution scale of our sampling may overestimate the actual distance because the minimum measurable distance is constrained to 30 m (from the center of one pixel to another) and previous research has shown that surviving trees may still occur within 30-m pixels classified as having burned severely (*52*).

Statistical analysis

We conducted a suite of analyses relating ROS with measures of wildfire impacts using linear and generalized linear mixed effects as implemented in the package glmmTMB (*86*). Because the distributions of ROS, daily area burned, and fire size are log-normal, we $\log_{10}$-transformed these variables in all models. We first explored relationships between linear ROS and daily area burned. We also related final fire size to the maximum ($\log_{10}$-transformed) daily linear ROS measured for that fire. Unique fire IDs nested within ecoregion were included as a random-effect term on the intercept in the model of daily area burned; only ecoregion was included as a random-effect term on the intercept in the model of final fire size. We calculated R^2 for these models using the method of Nakagawa *et al.* (*87*) as implemented by the MuMIn package (*88*).

We compared the distributions of each of the three postfire metrics (burn severity, proportion of patch area burned at high severity, and distance from high-severity patch interior to live conifer tree seed sources) produced by fast versus slow events, and tested for significant differences between fast and slow events using linear and generalized linear mixed-effects models. We also tested for relationships between continuous, $\log_{10}$-transformed ROS and each of the postfire metrics using linear and generalized linear mixed-effects models. Proportion of high-severity fire is constrained between 0 and 1, we modeled this response variable using ordered beta regression. Because CBI is constrained between 0 and 3, we rescaled it to between 0 and 1 and used an ordinal β error structure in this model as well. A Gaussian error structure was used in the seed-source distance model. Each of these models included fire ID nested within ecoregion as a random-effect term on both the model intercept and slope. We also contrasted models predicting wildfire effects using continuous ROS (m) from those using an areal measure (DOB area; ha). All analyses were conducted in R (*89*).

Supplementary Materials

This PDF file includes:
Tables S1 to S3

REFERENCES

1. P. Jain, Q. E. Barber, S. W. Taylor, E. Whitman, D. C. Acuna, Y. Boulanger, R. D. Chavardès, J. Chen, P. Englefield, M. Flannigan, M. P. Girardin, C. C. Hanes, J. Little, K. Morrison, R. S. Skakun, D. K. Thompson, X. Wang, M.-A. Parisien, Drivers and impacts of the record-breaking 2023 wildfire season in Canada. *Nat. Commun.* **15**, 6764 (2024).
2. C. X. Cunningham, G. J. Williamson, D. M. J. S. Bowman, Increasing frequency and intensity of the most extreme wildfires on Earth. *Nat. Ecol. Evol.* **8**, 1420–1425 (2024).

3. F. Tedim, V. Leone, M. Amraoui, C. Bouillon, M. R. Coughlan, G. M. Delogu, P. M. Fernandes, C. Ferreira, S. McCaffrey, T. K. McGee, J. Parente, D. Paton, M. G. Pereira, L. M. Ribeiro, D. X. Viegas, G. Xanthopoulos, Defining extreme wildfire events: Difficulties, challenges, and impacts. *Fire* **1**, 9 (2018).
4. J. K. Balch, V. Iglesias, A. L. Mahood, M. C. Cook, C. Amaral, A. DeCastro, S. Leyk, T. L. McIntosh, R. C. Nagy, The fastest-growing and most destructive fires in the US (2001 to 2020). *Science* **386**, 425–431 (2024).
5. J. D. Coop, S. A. Parks, C. S. Stevens-Rumann, S. M. Ritter, C. M. Hoffman, Extreme fire spread events and area burned under recent and future climate in the western USA. *Glob. Ecol. Biogeogr.* **31**, 1949–1959 (2022).
6. J. A. Balik, J. D. Coop, M. A. Krawchuk, C. E. Naficy, M.-A. Parisien, S. A. Parks, C. S. Stevens-Rumann, E. Whitman, Biogeographic patterns of daily wildfire spread and extremes across North America. *Front. For. Glob. Change* **7**, 1355361 (2024).
7. A. Duane, M. Castellnou, M. Bachfischer, L. Brotons, Fire rate of spread and growth rate in a set of 30 global wildfires: New evidence of extreme fire behavior. *J. Environ. Inform.* **44**, 87 (2024).
8. M. P. Harris, J. D. Coop, J. A. Balik, J. R. McFarland, S. A. Parks, C. S. Stevens-Rumann, Aspen impedes wildfire spread in southwestern United States landscapes. *Ecol. Appl.* **35**, e70061 (2025).
9. J. E. Keeley, Fire intensity, fire severity and burn severity: A brief review and suggested usage. *Int. J. Wildland Fire* **18**, 116–126 (2009).
10. G. M. Byram, "Combustion of forest fuels," in *Forest Fire: Control and Use*, K. P. Davis, Ed. (New York, McGraw-Hill, 1959), pp. 61–89.
11. R. M. Nelson, Byram derivation of the energy criterion for forest and wildland fires. *Int. J. Wildland Fire* **3**, 131–138 (1993).
12. W. C. Bessie, E. A. Johnson, The relative importance of fuels and weather on fire behavior in subalpine forests. *Ecology* **76**, 747–762 (1995).
13. Z. A. Holden, A. K. Swanson, M. Sadegh, C. H. Luce, E. Noonan-Wright, R. A. Parsons, Soil moisture is a stronger predictor of forest fire spread potential than weather in the U.S. Northern rocky mountains. *Geophys. Res. Lett.* **52**, e2025GL116248 (2025).
14. S. M. Hood, C. W. McHugh, K. C. Ryan, E. Reinhardt, S. L. Smith, Evaluation of a post-fire tree mortality model for western USA conifers. *Int. J. Wildland Fire* **16**, 679–689 (2007).
15. M. G. Turner, W. H. Romme, Landscape dynamics in crown fire ecosystems. *Landsc. Ecol.* **9**, 59–77 (1994).
16. C. A. Cansler, D. McKenzie, Climate, fire size, and biophysical setting control fire severity and spatial pattern in the northern Cascade Range, USA. *Ecol. Appl.* **24**, 1037–1056 (2014).
17. L. Collins, K. Morrison, M. S. Buonanduci, L. Guindon, B. J. Harvey, M.-A. Parisien, S. Taylor, E. Whitman, Extremely large fires shape fire severity patterns across the diverse forests of British Columbia, Canada. *Ecosphere* **16**, e70364 (2025).
18. J. R. McFarland, J. D. Coop, J. A. Balik, K. C. Rodman, S. A. Parks, C. S. Stevens-Rumann, Extreme fire spread events burn more severely and homogenize postfire landscapes in the Southwestern United States. *Glob. Change Biol.* **31**, e70106 (2025).
19. E. Orland, T. D. McCabe, Y. Chen, R. C. Scholten, Z. Becker, R. A. Loehman, J. T. Randerson, S. R. Coffield, T. Liu, A. N. Shiklomanov, K. Nelson, B. Peterson, M. B. Follette-Cook, D. C. Morton, Near real-time indicators of burn severity in the western U.S. from active fire tracking. *Fire Ecol.* **21**, 55 (2025).
20. S. A. Parks, J. D. Coop, K. T. Davis, Intensifying fire season aridity portends ongoing expansion of severe wildfire in Western US Forests. *Glob. Change Biol.* **31**, e70429 (2025).
21. B. Byrne, J. Liu, K. W. Bowman, M. Pascolini-Campbell, A. Chatterjee, S. Pandey, K. Miyazaki, G. R. van der Werf, D. Wunch, P. O. Wennberg, C. M. Roehl, S. Sinha, Carbon emissions from the 2023 Canadian wildfires. *Nature* **633**, 835–839 (2024).
22. A. P. Williams, B. Livneh, K. A. McKinnon, W. D. Hansen, J. S. Mankin, B. I. Cook, J. E. Smerdon, A. M. Varuolo-Clarke, N. R. Bjarke, C. S. Juang, D. P. Lettenmaier, Growing impact of wildfire on western US water supply. *Proc. Natl. Acad. Sci. U.S.A.* **119**, e2114069119 (2022).
23. E. J. McClure, J. D. Coop, C. H. Guiterman, E. Q. Margolis, S. A. Parks, Contemporary fires are less frequent but more severe in dry conifer forests of the southwestern United States. *Commun. Earth Environ.* **5**, 581 (2024).
24. A. M. Woolman, J. D. Coop, J. D. Shaw, J. DeMarco, Extent of recent fire-induced losses of ponderosa pine forests of Arizona and New Mexico, USA. *For. Ecol. Manage.* **520**, 120381 (2022).
25. V. Danneyrolles, R. D. Chavardès, M. P. Girardin, A. A. Ali, D. Arseneault, H. Asselin, A.-C. Bélisle, Y. Boucher, D. Cyr, I. Drobyshev, S. Erni, D. M. Gaboriau, S. Gauthier, F. Gennaretti, E. A. Johnson, C. P. S. Larsen, A. Leduc, M.-A. Parisien, J. Portier, Z. Shakeri, T. H. Wallenius, Y. Bergeron, Contextualizing recent increases in Canadian boreal wildfire activity: Decadal burn rates still within historical variability of the two past centuries. *Can. J. For. Res.* **55**, 1–12 (2025).
26. P. E. Higuera, B. N. Shuman, K. D. Wolf, Rocky Mountain subalpine forests now burning more than any time in recent millennia. *Proc. Natl. Acad. Sci. U.S.A.* **118**, e2103135118 (2021).
27. C. Haffey, T. D. Sisk, C. D. Allen, A. E. Thode, E. Q. Margolis, Limits to ponderosa pine regeneration following large high-severity forest fires in the United States Southwest. *Fire Ecol.* **14**, 143–163 (2018).
28. B. J. Harvey, D. C. Donato, M. G. Turner, High and dry: Post-fire tree seedling establishment in subalpine forests decreases with post-fire drought and large stand-replacing burn patches. *Glob. Ecol. Biogeogr.* **25**, 655–669 (2016).
29. N. G. Kiel, M. G. Turner, Where are the trees? Extent, configuration, and drivers of poor forest recovery 30 years after the 1988 Yellowstone fires. *For. Ecol. Manage.* **524**, 120536 (2022).
30. C. S. Stevens-Rumann, K. B. Kemp, P. E. Higuera, B. J. Harvey, M. T. Rother, D. C. Donato, P. Morgan, Evidence for declining forest resilience to wildfires under climate change. *Ecol. Lett.* **21**, 243–252 (2018).
31. K. T. Davis, M. D. Robles, K. B. Kemp, P. E. Higuera, T. Chapman, K. L. Metlen, J. L. Peeler, K. C. Rodman, T. Woolley, R. N. Addington, B. J. Buma, C. A. Cansler, M. J. Case, B. M. Collins, J. D. Coop, S. Z. Dobrowski, N. S. Gill, C. Haffey, L. B. Harris, B. J. Harvey, R. D. Haugo, M. D. Hurteau, D. Kulakowski, C. E. Littlefield, L. A. McCauley, N. Povak, K. L. Shive, E. Smith, J. T. Stevens, C. S. Stevens-Rumann, A. H. Taylor, A. J. Tepley, D. J. N. Young, R. A. Andrus, M. A. Battaglia, J. K. Berkey, S. U. Busby, A. R. Carlson, M. E. Chambers, E. K. Dodson, D. C. Donato, W. M. Downing, P. J. Fornwalt, J. S. Halofsky, A. Hoffman, A. Holz, J. M. Iniguez, M. A. Krawchuk, M. R. Kreider, A. J. Larson, G. W. Meigs, J. P. Roccaforte, M. T. Rother, H. Safford, M. Schaedel, J. S. Sibold, M. P. Singleton, M. G. Turner, A. K. Urza, K. D. Clark-Wolf, L. Yocom, J. B. Fontaine, J. L. Campbell, Reduced fire severity offers near-term buffer to climate-driven declines in conifer resilience across the western United States. *Proc. Natl. Acad. Sci. U.S.A.* **120**, e2208120120 (2023).
32. J. D. Coop, S. A. Parks, C. S. Stevens-Rumann, S. D. Crausbay, P. E. Higuera, M. D. Hurteau, A. Tepley, E. Whitman, T. Assal, B. M. Collins, K. T. Davis, S. Dobrowski, D. A. Falk, P. J. Fornwalt, P. Z. Fulé, B. J. Harvey, V. R. Kane, C. E. Littlefield, E. Q. Margolis, M. North, M.-A. Parisien, S. Prichard, K. C. Rodman, Wildfire-driven forest conversion in western North American landscapes. *Bioscience* **70**, 659–673 (2020).
33. A. Duane, M. Castellnou, L. Brotons, Towards a comprehensive look at global drivers of novel extreme wildfire events. *Clim. Change* **165**, 43 (2021).
34. C. Juang, A. Williams, J. Abatzoglou, J. Balch, M. Hurteau, M. Moritz, Rapid growth of large forest fires drives the exponential response of annual forest-fire area to aridity in the western United States. *Geophys. Res. Lett.* **49**, e2021GL097131 (2022).
35. X. Wang, J. Oliver, T. Swystun, C. C. Hanes, S. Erni, M. D. Flannigan, Critical fire weather conditions during active fire spread days in Canada. *Sci. Total Environ.* **869**, 161831 (2023).
36. J. T. Abatzoglou, A. P. Williams, Impact of anthropogenic climate change on wildfire across western US forests. *Proc. Natl. Acad. Sci. U.S.A.* **113**, 11770–11775 (2016).
37. B. M. Wotton, M. D. Flannigan, Length of the fire season in a changing climate. *For. Chron.* **69**, 187–192 (1993).
38. L. E. Queen, S. Dean, D. Stone, P. Jain, J. Renwick, N. Melia, Y. Imada, Fingerprint of anthropogenic climate change detected in long-term western North American fire weather trends. *Commun. Earth Environ.* **6**, 387 (2025).
39. X. Wang, K. Studens, M.-A. Parisien, S. W. Taylor, J.-N. Candau, Y. Boulanger, M. D. Flannigan, Projected changes in fire size from daily spread potential in Canada over the 21st century. *Environ. Res. Lett.* **15**, 104048 (2020).
40. B. E. Potter, D. McEvoy, Weather factors associated with extremely large fires and fire growth days. *Earth Interact.* **25**, 160–176 (2021).
41. D. D. B. Perrakis, M. G. Cruz, M. E. Alexander, C. C. Hanes, D. K. Thompson, S. W. Taylor, B. J. Stocks, Improved logistic models of crown fire probability in Canadian conifer forests. *Int. J. Wildland Fire* **32**, 1455–1473 (2023).
42. Z. Wu, H. S. He, L. Fang, Y. Liang, R. A. Parsons, Wind speed and relative humidity influence spatial patterns of burn severity in boreal forests of northeastern China. *Ann. For. Sci.* **75**, 66 (2018).
43. A. M. S. Smith, W. T. Tinkham, D. P. Roy, L. Boschetti, R. L. Kremens, S. S. Kumar, A. M. Sparks, M. J. Falkowski, Quantification of fuel moisture effects on biomass consumed derived from fire radiative energy retrievals. *Geophys. Res. Lett.* **40**, 6298–6302 (2013).
44. S. W. Taylor, B. M. Wotton, M. E. Alexander, G. N. Dalrymple, Variation in wind and crown fire behaviour in a northern jack pine black spruce forest. *Can. J. For. Res.* **34**, 1561–1576 (2004).
45. M. A. Finney, S. S. McAllister, A review of fire interactions and mass fires. *J. Combust.* **2011**, 548328 (2011).
46. A. J. Dowdy, M. D. Fromm, N. McCarthy, Pyrocumulonimbus lightning and fire ignition on Black Saturday in southeast Australia. *J. Geophys. Res. Atmospheres* **122**, 7342–7354 (2017).
47. N. P. Lareau, N. J. Nauslar, J. T. Abatzoglou, The Carr fire vortex: A case of pyrotornadogenesis? *Geophys. Res. Lett.* **45**, 13107–13115 (2018).
48. M. A. Krawchuk, S. L. Haire, J. Coop, M.-A. Parisien, E. Whitman, G. Chong, C. Miller, Topographic and fire weather controls of fire refugia in forested ecosystems of northwestern North America. *Ecosphere* **7**, 1–18 (2016).
49. K. C. Rodman, K. T. Davis, S. A. Parks, T. B. Chapman, J. D. Coop, J. M. Iniguez, J. P. Roccaforte, A. J. Sánchez Meador, J. D. Springer, C. S. Stevens-Rumann, M. T. Stoddard, A. E. M. Waltz, T. N. Wasserman, Refuge-yeah or refuge-nah? Predicting locations of forest resistance and recruitment in a fiery world. *Glob. Change Biol.* **29**, 7029–7050 (2023).

50. K. L. Shive, A. Wuenschel, L. J. Hardlund, S. Morris, M. D. Meyer, S. M. Hood, Ancient trees and modern wildfires: Declining resilience to wildfire in the highly fire-adapted giant sequoia. *For. Ecol. Manage.* **511**, 120110 (2022).
51. N. S. Gill, M. G. Turner, C. D. Brown, S. I. Glassman, S. L. Haire, W. D. Hansen, E. R. Pansing, S. B. St Clair, D. F. Tomback, Limitations to propagule dispersal will constrain postfire recovery of plants and fungi in western coniferous forests. *Bioscience* **72**, 347–364 (2022).
52. R. B. Walker, J. D. Coop, W. M. Downing, M. A. Krawchuk, S. L. Malone, G. W. Meigs, How much forest persists through fire? High-resolution mapping of tree cover to characterize the abundance and spatial pattern of fire refugia across mosaics of burn severity. *Forests* **10**, 782 (2019).
53. J. E. Keeley, J. G. Pausas, P. W. Rundel, W. J. Bond, R. A. Bradstock, Fire as an evolutionary pressure shaping plant traits. *Trends Plant Sci.* **16**, 406–411 (2011).
54. L. Lavoie, L. Sirois, Vegetation changes caused by recent fires in the northern boreal forest of eastern Canada. *J. Veg. Sci.* **9**, 483–492 (1998).
55. A. H. Lloyd, C. L. Fastie, H. Eisen, Fire and substrate interact to control the northern range limit of black spruce (*Picea mariana*) in Alaska. *Can. J. For. Res.* **37**, 2480–2493 (2007).
56. D. Arseneault, Impact of fire behavior on postfire forest development in a homogeneous boreal landscape. *Can. J. For. Res.* **31**, 1367–1374 (2001).
57. N. S. Gill, T. J. Hoecker, M. G. Turner, The propagule doesn't fall far from the tree, especially after short-interval, high-severity fire. *Ecology* **102**, e03194 (2021).
58. M. R. Kreider, L. L. Yocom, Aspen seedling establishment, survival, and growth following a high-severity wildfire. *For. Ecol. Manage.* **493**, 119248 (2021).
59. C. H. Guiterman, E. Q. Margolis, C. D. Allen, D. A. Falk, T. W. Swetnam, Long-term persistence and fire resilience of oak shrubfields in dry conifer forests of Northern New Mexico. *Ecosystems* **21**, 943–959 (2018).
60. P. García-Llamas, S. Suárez-Seoane, A. Taboada, A. Fernández-Manso, C. Quintano, V. Fernández-García, J. M. Fernández-Guisuraga, E. Marcos, L. Calvo, Environmental drivers of fire severity in extreme fire events that affect Mediterranean pine forest ecosystems. *For. Ecol. Manage.* **433**, 24–32 (2019).
61. S. A. Parks, L. M. Holsinger, M. H. Panunto, W. M. Jolly, S. Z. Dobrowski, G. K. Dillon, High-severity fire: Evaluating its key drivers and mapping its probability across western US forests. *Environ. Res. Lett.* **13**, 044037 (2018).
62. M. R. Kreider, P. E. Higuera, S. A. Parks, W. L. Rice, N. White, A. J. Larson, Fire suppression makes wildfires more severe and accentuates impacts of climate change and fuel accumulation. *Nat. Commun.* **15**, 2412 (2024).
63. J. L. Baltzer, N. J. Day, X. J. Walker, D. Greene, M. C. Mack, H. D. Alexander, D. Arseneault, J. Barnes, Y. Bergeron, Y. Boucher, L. Bourgeau-Chavez, C. D. Brown, S. Carrière, B. K. Howard, S. Gauthier, M.-A. Parisien, K. A. Reid, B. M. Rogers, C. Roland, L. Sirois, S. Stehn, D. K. Thompson, M. R. Turetsky, S. Veraverbeke, E. Whitman, J. Yang, J. F. Johnstone, Increasing fire and the decline of fire adapted black spruce in the boreal forest. *Proc. Natl. Acad. Sci. U.S.A.* **118**, e2024872118 (2021).
64. K. T. Davis, S. Z. Dobrowski, P. E. Higuera, Z. A. Holden, T. T. Veblen, M. T. Rother, S. A. Parks, A. Sala, M. P. Maneta, Wildfires and climate change push low-elevation forests across a critical climate threshold for tree regeneration. *Proc. Natl. Acad. Sci. U.S.A.* **116**, 6193–6198 (2019).
65. B. Buma, S. Weiss, K. Hayes, M. Lucash, Wildland fire reburning trends across the US West suggest only short-term negative feedback and differing climatic effects. *Environ. Res. Lett.* **15**, 034026 (2020).
66. A. J. Tepley, X. Wang, M. D. Flannigan, M.-A. Parisien, A negative fire–vegetation feedback substantially limits reburn extent across the North American boreal biome. *Ecosystems* **28**, 62 (2025).
67. A. J. Tepley, E. Thomann, T. T. Veblen, G. L. W. Perry, A. Holz, J. Paritsis, T. Kitzberger, K. J. Anderson-Teixeira, Influences of fire–vegetation feedbacks and post-fire recovery rates on forest landscape vulnerability to altered fire regimes. *J. Ecol.* **106**, 1925–1940 (2018).
68. E. Whitman, Q. E. Barber, P. Jain, S. A. Parks, L. Guindon, D. K. Thompson, M.-A. Parisien, A modest increase in fire weather overcomes resistance to fire spread in recently burned boreal forests. *Glob. Change Biol.* **30**, e17363 (2024).
69. S. McCaffrey, Community wildfire preparedness: A global state-of-the-knowledge summary of social science research. *Curr. For. Rep.* **1**, 81–90 (2015).
70. B. E. Law, J. T. Abatzoglou, C. R. Schwalm, D. Byrne, N. Fann, N. J. Nassikas, Anthropogenic climate change contributes to wildfire particulate matter and related mortality in the United States. *Commun. Earth Environ.* **6**, 336 (2025).
71. M. Sample, A. E. Thode, C. Peterson, M. R. Gallagher, W. Flatley, M. Friggens, A. Evans, R. Loehman, S. Hedwall, L. Brandt, M. Janowiak, C. Swanston, Adaptation strategies and approaches for managing fire in a changing climate. *Climate* **10**, 58 (2022).
72. K. T. Davis, J. Peeler, J. Fargione, R. D. Haugo, K. L. Metlen, M. D. Robles, T. Woolley, Tamm review: A meta-analysis of thinning, prescribed fire, and wildfire effects on subsequent wildfire severity in conifer dominated forests of the Western US. *For. Ecol. Manage.* **561**, 121885 (2024).
73. C. D. Crouch, P. C. Rogers, M. M. Moore, K. M. Waring, Building ecosystem resilience and adaptive capacity: A systematic review of aspen ecology and management in the southwest. *For. Sci.* **69**, 334–354 (2023).
74. S. Z. Dobrowski, M. M. Aghai, A. C. du Lac, R. Downer, J. Fargione, D. L. Haase, T. Hoecker, O. A. Kildisheva, A. Murdoch, S. Newman, M. P. North, P. Saksa, M. Sjoholm, T. Baribault, M. S. Buonanduci, M. E. Chambers, L. Gonzales-Kramer, B. J. Harvey, M. D. Hurteau, J. Loevner, H. D. Safford, J. Sloan, 'Mind the Gap'—Reforestation needs vs. reforestation capacity in the western United States. *Front. For. Glob. Change* **7**, 1402124 (2024).
75. R. C. Rothermel, A mathematical model for predicting fire spread in wildland fuels, in *Intermountain Forest & Range Experiment Station, Forest Service* (US Department of Agriculture, 1972), vol. 115.
76. Commission for Environmental Cooperation, 1997. Ecological regions of North America: Toward a common perspective. The Commission.
77. LANDFIRE, 2022. LANDFIRE 200 US Dep. Inter. Geol. Surv. US Dep. Agric.
78. T. Hermosilla, M. A. Wulder, J. C. White, N. C. Coops, G. W. Hobart, Disturbance-informed annual land cover classification maps of Canada's forested ecosystems for a 29-year landsat time series. *Can. J. Remote Sens.* **44**, 67–87 (2018).
79. J. Eidenshink, A project for monitoring trends in burn severity. *Fire Ecol.* **3**, 3–21 (2007).
80. Canadian Forest Service, National Burned Area Composite (NBAC). Natural Resources Canada, Canadian Forest Service (Northern Forestry Centre, Edmonton, Alberta, 2024); https://cwfis.cfs.nrcan.gc.ca.
81. S. A. Parks, Mapping day-of-burning with coarse-resolution satellite fire-detection data. *Int. J. Wildland Fire* **23**, 215–223 (2014).
82. N. Gorelick, M. Hancher, M. Dixon, S. Ilyushchenko, D. Thau, R. Moore, Google earth engine: Planetary-scale geospatial analysis for everyone. *Remote Sens. Environ.* **202**, 18–27 (2017).
83. S. A. Parks, L. M. Holsinger, M. J. Koontz, L. Collins, E. Whitman, M.-A. Parisien, R. A. Loehman, J. L. Barnes, J.-F. Bourdon, J. Boucher, Y. Boucher, A. C. Caprio, A. Collingwood, R. J. Hall, J. Park, L. B. Saperstein, C. Smetanka, R. J. Smith, N. Soverel, Giving ecological meaning to satellite-derived fire severity metrics across North American forests. *Remote Sens.* **11**, 1735 (2019).
84. C. Key, N. Benson, "Landscape assessment: Remote sensing of severity, the normalized burn ratio and ground measure of severity, the composite burn index." in *FIREMON Fire Effect Monitoring and Inventory System* (USDA Forest Service, Rocky Mountain Research Station, Ogden, Utah, 2005).
85. J. D. Miller, E. E. Knapp, C. H. Key, C. N. Skinner, C. J. Isbell, R. M. Creasy, J. W. Sherlock, Calibration and validation of the relative differenced Normalized Burn Ratio (RdNBR) to three measures of fire severity in the Sierra Nevada and Klamath Mountains, California, USA. *Remote Sens. Environ.* **113**, 645–656 (2009).
86. M. E. Brooks, K. Kristensen, K. J. van Benthem, A. Magnusson, C. W. Berg, A. Nielsen, H. J. Skaug, M. Mächler, B. M. Bolker, glmmTMB balances speed and flexibility among packages for zero-inflated generalized linear mixed modeling. *R J.* **9**, 378–400 (2017).
87. S. Nakagawa, P. C. D. Johnson, H. Schielzeth, The coefficient of determination R^2 and intra-class correlation coefficient from generalized linear mixed-effects models revisited and expanded. *J. R. Soc. Interface* **14**, 20170213 (2017).
88. K. Bartoń, *MuMIn: Multi-Model Inference*. R package version 1.48.19 (2026); https://CRAN.R-project.org/package=MuMIn.
89. R Core Team, R: A Language and Environment for Statistical Computing. R Foundation for Statistical Computing, (Vienna, Austria, 2025); https://www.scirp.org/reference/referencespapers?referenceid=3967248.

Acknowledgments: J.D.C., S.A.P., and C.S.S.-R. also thank Tall Timbers for hosting a productive writing retreat. **Funding:** Funding support for this research was provided to CSSR and JDC by the Southwest Climate Adaptation Science Center (678348), and to J.D.C. by the USDA Forest Service Western Wildland Environmental Threat Assessment Center via an agreement between the Rocky Mountain Research Station and Western Colorado University (22-CS-11221639-139). J.R.M. was also supported by the National Science Foundation Research Traineeship Program (NSF-NRT; award no. 2125921). **Author contributions:** Conceptualization: J.D.C., J.A.B., J.R.M., S.A.P., C.S.S.-R., M.A.K., C.E.N., and E.W. Data curation: J.D.C. and S.A.P.. Formal analysis: J.D.C. and J.A.B.. Funding acquisition: J.D.C., C.S.S.-R., S.A.P., and C.E.N. Investigation: J.D.C., J.A.B., J.R.M., and S.A.P. Methodology: J.D.C., J.A.B., J.R.M., S.A.P., C.S.S.-R., K.C.R., and E.W. Project administration: J.D.C. and C.S.S.-R. Resources: S.A.P. Software: J.A.B. Supervision: J.D.C. Validation: J.A.B. Visualization: J.D.C. and J.A.B. Writing–original draft: J.D.C., C.S.S.-R., M.A.-P., and E.W. Writing–review and editing: J.D.C., J.A.B., J.R.M., S.A.P., K.C.R., C.S.S.-R., M.A.K., C.E.N., M.A.-P., and E.W. **Competing interests:** The authors declare that they have no competing interests. **Data, code, and materials availability:** All data and code needed to evaluate and reproduce the results in the paper will be made available upon publication in the following Dryad repository: https://doi.org/10.5061/dryad.rjdfn2zsp. This study did not generate new materials.

Submitted 18 February 2026
Accepted 1 July 2026
Published 12 August 2026
10.1126/sciadv.aeg5802